



Temperature characteristics and heat load in the City of Dubrovnik

Marijana Boras ¹, Ivana Herceg-Bulić ¹, Matej Žgela ¹
and Irena Nimac ^{2,3}

¹Department of Geophysics, Faculty of Science, University of Zagreb, Zagreb, Croatia

²Meteorological and Hydrological Service of Croatia, Zagreb, Croatia

³Wegener Center für Klima und Globalen Wandel, University of Graz, Graz, Austria

Received 9 June 2022, in final form 10 October 2022

In this study, temperature characteristics and heat load in the city of Dubrovnik are investigated by using temperature data observed at the local meteorological station in Dubrovnik for the period 1961–2019, satellite data collected by LANDSAT5 satellite for the period 2001–2010, and climate indices data obtained from simulations of an urban climate model (MUKLIMO_3) for the period 2001–2010. Trends in daily mean, maximum, minimum, and seasonal temperatures were analysed by using Sen's slope and the Mann-Kendall test. Results reveal rising trends for all of the studied temperature-related elements. However, it is demonstrated that temperature increase is greatest for the summer season with the highest rise for daily maximum temperatures. The same approach was applied to examine trends of climate indices (summer days and tropical nights), which indicates an increase in the number of both summer days and tropical nights. Results of satellite data of average summer land surface temperatures for the period 2001–2010 indicate that urbanised surfaces and bare rock areas heat up more than natural surfaces with vegetation. Climate indices (summer and hot days, warm evenings, and tropical nights) simulated by the urban climate model MUKLIMO_3 also reveal that, on average, in the city of Dubrovnik urbanised surfaces heat up more than natural surfaces with vegetation and that nocturnal heat load is reduced in lower-density built-up areas.

Keywords: temperature, heat load, urban climate, Sen's slope, Mann-Kendall test, climate indices, model MUKLIMO_3, satellite LANDSAT5

1. Introduction

Public awareness of climate change in the entire world is rising, mainly due to more frequent extreme weather events, such as heatwaves, droughts, and extreme precipita-

tion. Furthermore, it is predicted that the frequency and intensity of extreme weather events will increase in the future (IPCC, 2021).

Recently more attention has been dedicated to climate conditions in urban areas because of their particular meteorological and climatic characteristics and the fact that more than half of the world's population lives in cities. Interaction between the atmosphere and urban areas results in specific climate conditions – urban climate (Oke et al., 2017). In urban areas, original natural surfaces have been converted into surfaces made from artificial materials (concrete, asphalt, etc.), absorbing and retaining heat more than natural materials. Additionally, urban covers are mainly made from impervious materials, which increase the flood risk associated with extreme precipitation. Further, according to the complex spatial structure of cities, radiative cooling is diminished, and heat storage is enhanced due to the vast number of artificial surfaces that are in contact with the atmosphere. Therefore, air temperature is significantly higher in cities than in surrounding rural areas, especially during the night and during clear anticyclonic weather conditions. This effect is known as an urban heat island (UHI). In cases of low wind speeds, UHI can induce phenomena similar to sea-land breeze circulation, with air flowing from the surrounding region toward the city. Some such cases are accompanied by the recirculation of pollution affecting air quality in the city (Masson et al., 2020).

Besides temperature changes, cities affect wind characteristics too. The roughness of urban surfaces provokes wind deceleration due to friction force (Klaić et al., 2002). This is particularly evident for strong and moderate winds, for which besides the wind deceleration, slight turning in the pressure gradient direction is occurring. In cases of divergence or convergence, vertical motion is possible as well. Cities emit vast amounts of greenhouse gases. However, Balling et al. (2001) state that these concentrations inappreciably contribute to the creation of UHI. Temperature enhancement in urban areas is caused mainly by drier soils and heat-absorbing materials. Even though greenhouse gases emitted by cities do not contribute to the creation of UHI, they support global climate warming to which cities are exposed as well. Global warming is manifested in many processes that affect urban climate, like temperature rise, and increased occurrence of extreme weather events such as heat waves, changes in the regime of precipitation, severe weather, etc. (Masson et al., 2020).

As was previously mentioned, temperature increase in cities is caused by global warming, and at the same time, it can be enhanced by cities' morphological structure. For example, extreme weather events such as heat waves are more intensive in urban areas (Tan et al., 2010) making particularly unpleasant climate conditions for dwellers. Since about half of the world's population lives in cities, with a tendency to rise even more (UN, 2019), further research on urban climate is indispensable. In general, cities are very complex structures. Each city has unique morphological, geographical, economic, and other features. Consequently, when researching possibilities and ways of mitigation of the UHI and global warming effects in urban areas, an individual approach is required.

In this study, the temperature features of the city of Dubrovnik are investigated. Dubrovnik is situated in the south of Croatia (42° 38' 53" N, 18° 5' 32" E) on the southern Adriatic Sea coast and westward of the mountain barrier. This position is geographically interesting (*i.e.* land-sea distribution) and Dubrovnik's relatively small urban area is influenced by different climate factors, like sea-land breeze circulation and mountain-valley breeze circulation. Some studies indicate that sea surface temperatures in the

eastern Adriatic have positive trends of growth in the period 1952–2010 (Vilibić et al., 2013), while others state that the warming of the sea in Adriatic has even amplified since 2008 (Grbec et al., 2018). These temperature changes could influence cities' climate characteristics as well. According to Köppen-Geiger's climate classification, the climate in Dubrovnik belongs to the hot-summer Mediterranean type. In 1971–2000, the highest maximum daily temperature was in July and August (35.5 °C and 36.7 °C), while the minimum daily temperature in these months was 14.1 °C. Maximum daily temperatures in spring and autumn were higher than 23 °C, while in the winter months, January and February, the mean daily temperature was about 9 °C. Snow is an exceedingly rare phenomenon. According to the annual wind rose, the strongest wind in Dubrovnik is bora, which blows from the northeast (Zaninović et al., 2008).

The city of Dubrovnik is located in the Mediterranean region, which is recognised as a hot spot, meaning it is very vulnerable and reacts fast to climate changes. The effects of climate change in this region are extreme for the environment and economic activities (Giorgi, 2006). The importance of examining temperature characteristics and heat load in this place is recognised since Dubrovnik is a Mediterranean city, and one of the most important economic industries here, tourism, is very vulnerable to climate change too (Jopp et al., 2010). Famous Old City in Dubrovnik and its wonderful nature attract tourists during the whole year, but most tourists come in the summer when negative and unpleasant climate conditions are strongly manifested. This study is intended to examine temperature characteristics and heat load in the city of Dubrovnik by utilising three different approaches. First, observed temperature data from the local meteorological station for the period 1961–2019 was analysed to examine trends in temperature and climate indices. Afterwards, to estimate the spatial pattern of the heat load in Dubrovnik according to Land Use/Land Cover (LULC) classification, satellite data, and simulations of model Microscale Urban Climate Model in three dimensions (MUKLIMO_3) were used. Climate indices were calculated from observed temperature data to estimate temporal temperature changes. Climate indices obtained from the MUKLIMO_3 were calculated to estimate the spatial distribution of the heat load in the city, *i.e.*, which parts of the town are more heated and does the density of built-up make any difference in the distribution of heat load. These three different approaches are used to obtain an overall analysis of temperature characteristics and heat load in the city of Dubrovnik.

2. Data and methods

2.1. Observed temperature data analysis

Observed temperature data at the local meteorological station in Dubrovnik used in this study were obtained from the Croatian Meteorological and Hydrological Service for the period 1.1.1961–31.12.2019. Daily data of temperature values at 07, 14, and 21 h, minimum daily and maximum daily temperature data were utilised for examining temperature trends and calculating climate indices. Data of minimum and maximum daily temperature were missing in the period 22.3.1978–13.5.1979, therefore, they could not be included in the analysis. Furthermore, the time series of temperature values at 07, 14, and 21 h were not complete in 1978, so data for this year could not be included in the analysis too. The observed data used in this work were collected at one of the main meteorological stations of the Meteorological and Hydrological Service of Croatia, where

standardized measurements and data quality checks are carried out. Therefore, even though there are missing data during 1978–1979, which is probably a consequence of the relocation of the meteorological station, which did not lead to a break in the data homogeneity (Pandžić and Likso, 2010), the data used in this paper can be considered relevant (Nimac and Perčec Tadić, 2017). Other possible causes of inhomogeneity, such as urbanization, were not removed in order to investigate their influence on changes in temperature characteristics.

Mean daily temperature is calculated by using the relation

$$t = \frac{t_{07} + t_{14} + 2t_{21}}{4}$$

where t is the mean daily temperature and t_{07} , t_{14} , and t_{21} are temperature values measured at 7, 14, and 21 h. The annually-averaged mean daily temperatures (hereinafter mean daily temperatures) are mean daily temperatures averaged for every year, while mean seasonal (hereinafter, seasonal) daily temperatures are daily (mean, minimum, or maximum) temperatures averaged for a specific season for every year. In this work, an analysis of all of the four seasons is made: spring (MAM, *March April May*), summer (JJA, *June July August*), autumn (SON, *September October November*), and winter (DJF, *December January February*).

In addition, daily temperature extremes (maximum and minimum daily temperature) were used to examine climate extremes in Dubrovnik by calculating climate indices, precisely summer days and tropical nights. According to the recommendations of the World Meteorological Organisation, a set of climate indices standardised by the CCI/WCRP/JCOMM Expert Team on Climate Change Detection and Indices (ETCCDI), which are related to temperature and precipitation data, should be utilised for analysis of climate extremes (WMO, 2004). These indices, standardised to have comparable data worldwide, are used for analysing temporal and spatial changes in the occurrence of weather extremes (such as heat waves, and cold waves). In the present study, Climdex climate indices were calculated. According to the Climdex climate indices (a standardised set of indices recommended by the ETCCDI), climate indices summer days are defined as days per year with a maximum daily temperature higher than 25 °C ($T_x > 25$ °C), while the annual number of tropical nights is obtained by counting days per year with a minimum daily temperature higher than 20 °C ($T_n > 20$ °C) (Climdex, 2020).

Sen's slope (Sen, 1968) and Mann-Kendall test were applied to examine temporal temperature changes by estimating linear trends and their statistical significance at a 5% significance level (Mann, 1945; Kendall, 1975). Data preparation, trend analysis, and graphical presentations of results were carried out in *Python* using *matplotlib*, *matplotlib.pyplot*, and *pymannkendall* packages.

2.2. Model MUKLIMO_3 and model set up for Dubrovnik

In this study, the Microscale Urban Climate Model in three dimensions (MUKLIMO_3) (Sievers and Zdunkowski, 1986; Sievers, 1990, 1995) is used to explore urban heat load in the city of Dubrovnik and the surface influence on the spatial distribution of the heat load by simulating atmospheric conditions in Dubrovnik for the period 2001–2010. For this purpose, a set of climate indices was calculated using the cuboid method based

on the results of MUKLIMO_3 simulations and climatological data from the local meteorological station.

MUKLIMO_3 is a model in which atmospheric temperature fields are simulated by solving Reynolds-averaged Navier-Stokes (RANS) equations, prognostic temperature equation, and prognostic humidity equations while considering soil heat capacity, possibilities of moisture storage in soil, and a sophisticated vegetation model. These temperature fields are simulated in an urban environment with particular emphasis on the interaction between the atmosphere and buildings (Früh et al., 2011). The model is first driven by a set of initial air temperature, wind speed, and relative humidity to obtain the 1D profile of these parameters, which then serve as initial conditions for 3D model simulations. The cuboid method, used in this study for estimating climate indices over a longer period, is based on trilinear interpolation among cuboid corners defined by thresholds (minimum and maximum values) for air temperature, relative humidity, and wind speed data for which it is estimated that occurrence of the heat load situations in the city is most likely. Here, the threshold used is $T_{min} = 15$ °C. In the cuboid method, simulations of MUKLIMO_3 model of the daily cycle for each of the eight cuboid corners for two prevailing wind directions are done first. Furthermore, considering climatic data from the local station for a specific day (air temperature, relative humidity, wind speed and wind direction data), weighting factors are calculated for each cuboid corner and applied to trilinear interpolation. The trilinear interpolation yields interpolated fields of air temperature, relative humidity, and wind speed which enable the calculation of the spatial distribution of climate indices. A more detailed description of the MUKLIMO_3 model and the cuboid method can be found in several studies considering urban heat load (Früh et al., 2011; Žuvela-Aloise et al., 2014, 2016; Žuvela-Aloise, 2017; Nimac et al., 2022).

In this study, in the cuboid method, climate indices of summer days (days with maximum daily temperature $T_x \geq 25$ °C), hot days (days with maximum daily temperature $T_x \geq 30$ °C), warm evenings (days with the temperature at 20 h according to Central European Summer Time $T_{20} \geq 20$ °C), and tropical nights (days with minimum daily temperature $T_n \geq 20$ °C) are calculated from simulated data. The model domain covers an area of 6.8 km × 5.2 km with a 100 m horizontal resolution (Fig. 1a). Input data for the MUKLIMO_3 model is the terrain file and the land use/ land cover (LULC) file made according to the morphological city structure from 2012 (Fig. 1b). Input for the cuboid method was the data from the local meteorological station in Dubrovnik for the period 2001–2010. Model simulations were performed for the two prevailing wind directions, northeast (NE) and southwest (SW). From given interpolated temperature fields, for the period 2001–2010, annually-averaged climate indices were calculated. This period is selected for simulations to be in accordance with the used LULC classification. Modelling results are processed and visually depicted using the Geographic Information System (GIS) and *Python* programming language. Annually-averaged numbers of days for the climate indices for the period 2001–2010 are visually demonstrated on the domain area (with 100 m horizontal resolution) using GIS, while the analysis of climate indices according to LULC classes for the period 2001–2010 is performed utilizing *Python*, precisely, *matplotlib* package.

2.3. Satellite data analysis

Satellite data utilised in this study were recorded by the LANDSAT5 satellite (Sorbrino et al., 2004). This data is used to obtain the spatial distribution of the heat load in

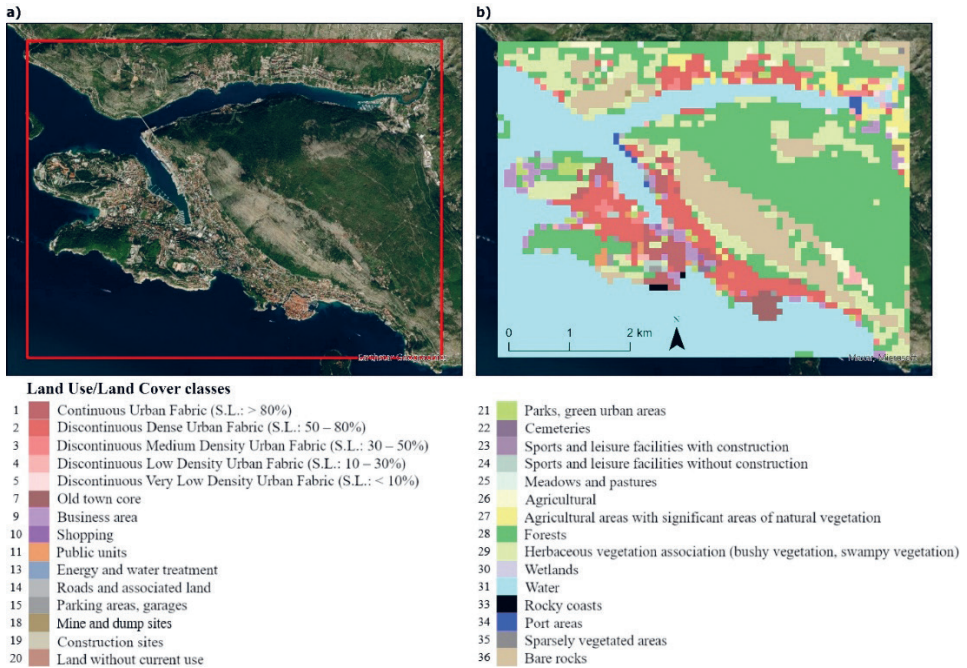


Figure 1. *a)* Satellite view of Dubrovnik area, red framework encompasses model domain. *b)* Land use/land cover distribution with a description of LULC classification.

the city of Dubrovnik by calculating the average summer land surface temperature. All available data for the JJA season in 2001–2010 were used to get the average summer land surface temperature (hereinafter LST). LST is selected because temperatures in Dubrovnik are the highest in the summertime and, therefore, the heat load as well. Google Earth Engine (GEE) online platform is employed for processing satellite images, while the results were visualised using GIS. GEE is an online platform specialising in geospatial data analysis. It is based on its cloud data storage and provides different functions within the *Javascript* programming language for analysing satellite images (Graczyk et al., 2017). In this study, the code for the analysis was created in *Javascript* likewise. The derived distribution of LST is aggregated to 100 m spatial resolution and depicted on the same domain as the MUKLIMO_3, so satellite data and MUKLIMO_3 modelled data to be comparable.

3. Results

3.1. Measured data

Firstly, measured temperature data from the meteorological station in Dubrovnik for the period 1961–2019, is processed to analyse temperature characteristics in the city of Dubrovnik.

3.1.1. Air temperature trend

Annually-averaged mean daily temperatures (hereinafter, mean daily temperatures) in 1961–2019 are presented in Fig. 2. Besides the fluctuations of mean daily temperatures, its increase is evident. Linear trends of temperature for 30-year climatic periods are calculated using Sen's slope to investigate and inspect the characteristics of this growth. Obtained trends depict a mild descending trend of mean daily temperature for the first period (1961–1990), while there are increasing temperature trends in the following periods. According to Mann-Kendall (hereinafter MK) test, in the time series 1961–1990, there is no statistically significant trend ($p_{(1961-1990)} = 0.335$). However, for the following periods, the MK test indicates that statistically significant trends exist ($p_{(1971-2000)} = 0.008$, $p_{(1981-2010)} = 0.003$, $p_{(1991-2019)} < 0.001$, $p_{(1961-2019)} < 0.001$). Sen's slope shows that mean daily temperature increases in all observed periods except for the first one (1961–1990). Derived linear trends are positive and indicate that the mean daily temperature in Dubrovnik has been rising during the last 50 years. The increase in mean daily temperature for 1961–2019 is equal to $0.28 \text{ } ^\circ\text{C} (10\text{y})^{-1}$. However, temperature trends over 30-year periods show increasing amounts of temperature growth. In the period 1971–2000, the increase in mean daily temperature was equal to $0.29 \text{ } ^\circ\text{C} (10\text{y})^{-1}$, in the next period it was $0.37 \text{ } ^\circ\text{C} (10\text{y})^{-1}$, while in the last period, 1991–2019, it was equal to $0.57 \text{ } ^\circ\text{C} (10\text{y})^{-1}$. Therefore, it can be concluded that the temperature growth is accelerating in Dubrovnik.

Previous results indicate an accelerating increase in daily temperature in Dubrovnik. However, the temperature is not expected to rise equally in all seasons. Therefore, temperature changes for different seasons are shown as well (Fig. 3). The greatest growth is obtained for the JJA season ($0.43 \text{ } ^\circ\text{C} (10\text{y})^{-1}$), for which the highest mean daily temperatures are already expected. The smallest growth of mean seasonal temperatures is attained for the SON season ($0.12 \text{ } ^\circ\text{C} (10\text{y})^{-1}$), and DJF season ($0.13 \text{ } ^\circ\text{C} (10\text{y})^{-1}$), while in the MAM season linear trend is equal to ($0.29 \text{ } ^\circ\text{C} (10\text{y})^{-1}$). MK test demonstrates that in all observed periods, except for the SON season, there are statistically significant trends

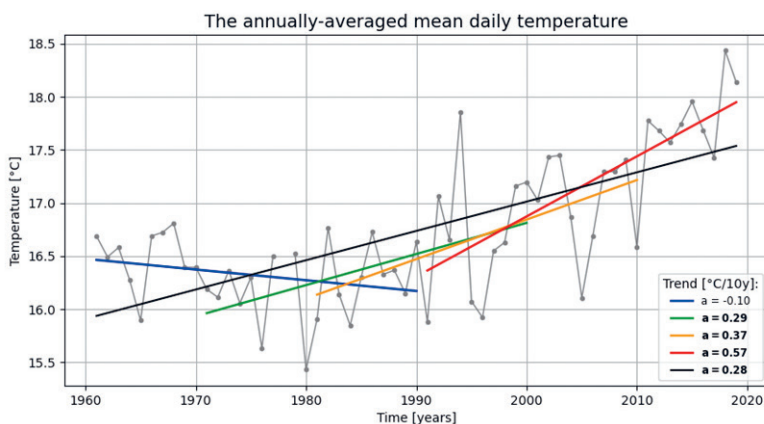


Figure 2. Trends for the period 1961–2019 (*black*) and trends of 30-year climatologic periods for annually-averaged mean daily temperatures observed at the meteorological station in Dubrovnik. From left to right beginning with the time period 1961–1990 (*blue*), 1971–2000 (*green*), 1981–2010 (*orange*) and 1991–2019 (*red*). In legend are given Sen's slope results ($^\circ\text{C} (10\text{y})^{-1}$) and in bold is designated if according to the MK test in the given period statistically significant trend exists.

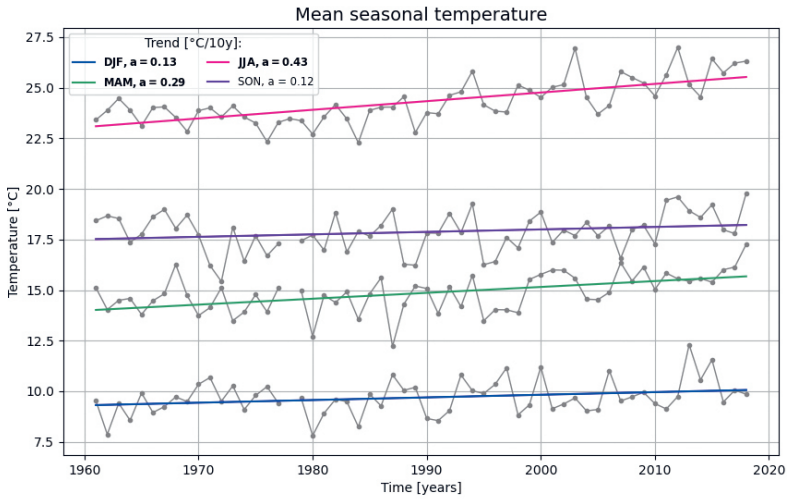


Figure 3. Trends for mean seasonal temperatures observed at the meteorological station in Dubrovnik for the period 1961–2018. In legend are given Sen's slope results ($^{\circ}\text{C} (10\text{y})^{-1}$) and in bold is designated if according to the MK test in a given time statistically significant trend exists.

($p_{DJF} = 0.041$, $p_{MAM} < 0.001$, $p_{JJA} < 0.001$, $p_{SON} = 0.088$). Furthermore, the obtained trends are positive for all seasons, implying that mean daily temperatures are rising in all seasons with the strongest warming in the summer season.

Changes in extreme temperatures (minimum and maximum daily temperature) are also important indicators of climate change. In the observed period 1961–2018, a positive trend of maximum daily temperature is obtained in every season (Fig. 4). From the graph

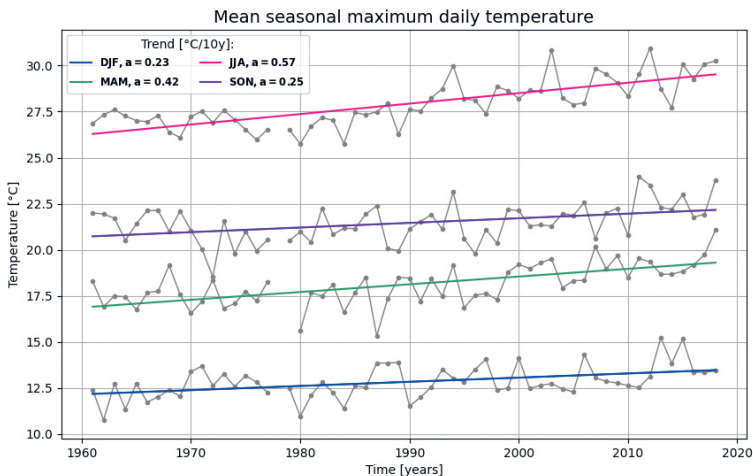


Figure 4. Trends for mean seasonal maximum daily temperatures observed at the meteorological station in Dubrovnik for the period 1961–2018. In legend are given Sen's slope results ($^{\circ}\text{C} (10\text{y})^{-1}$) and in bold is designated if according to the MK test in a given time statistically significant trend exists.

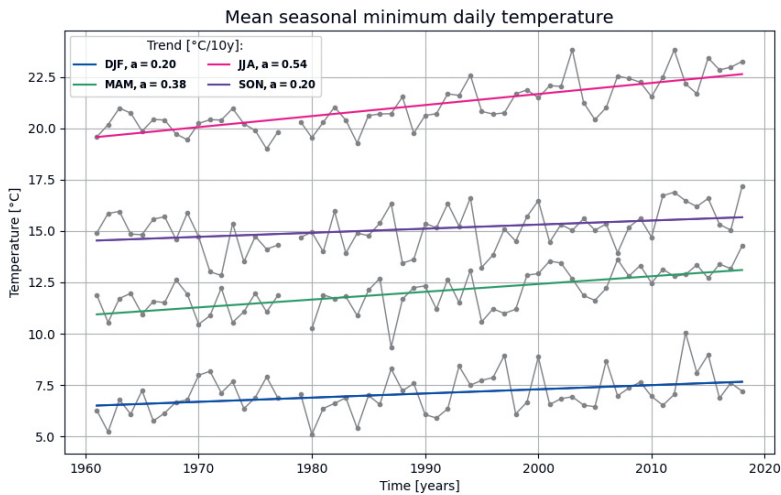


Figure 5. Trends for mean seasonal minimum daily temperatures observed at the meteorological station in Dubrovnik for the period 1961–2018. In legend are given Sen's slope results ($^{\circ}\text{C} (10\text{y})^{-1}$) and in bold is designated if according to the MK test in a given time statistically significant trend exists.

it is visible that the greatest trend increase corresponds to the JJA season ($0.57\text{ }^{\circ}\text{C} (10\text{y})^{-1}$), followed by a trend in the MAM season ($0.42\text{ }^{\circ}\text{C} (10\text{y})^{-1}$), then for the SON ($0.25\text{ }^{\circ}\text{C} (10\text{y})^{-1}$) and DJF seasons ($0.23\text{ }^{\circ}\text{C} (10\text{y})^{-1}$). According to the MK test for mean seasonal maximum daily temperatures, a statistically significant trend exists in every season in the observed period ($p_{DJF} = 0.000$, $p_{MAM} < 0.001$, $p_{JJA} < 0.001$, $p_{SON} = 0.004$).

For seasonal minimum daily temperatures (Fig. 5), as well as for mean seasonal maximum daily temperature, results of the MK test indicate that a statistically significant trend exists in every season ($p_{DJF} = 0.006$, $p_{MAM} < 0.001$, $p_{JJA} < 0.001$, $p_{SON} = 0.013$). From Sen's slope results, it is visible that in the entire observed period, minimum daily temperatures rise in all seasons. As in the two previous cases, the strongest positive trend is obtained for the JJA season ($0.54\text{ }^{\circ}\text{C} (10\text{y})^{-1}$). The MAM season follows with a trend equal to ($0.38\text{ }^{\circ}\text{C} (10\text{y})^{-1}$), while the SON and DJF seasons have equal trends of ($0.20\text{ }^{\circ}\text{C} (10\text{y})^{-1}$).

3.1.2. Climate indices trend

From the previous results of seasonal extreme daily temperatures, it is evident that maximum and minimum daily temperatures are rising. Extreme daily temperatures affect significantly the quality of life in urban areas, therefore considering climate indices based on minimum daily and maximum daily temperature provides convenient insight into the estimation of urban heat load strength. In this work, temporal changes in climate indices of summer days ($T_x > 25\text{ }^{\circ}\text{C}$) and tropical nights are analysed ($T_n > 20\text{ }^{\circ}\text{C}$).

The warming of the city is reflected in the annual number of summer days (Fig. 6). Statistically significant trends in observed data are confirmed by the MK test for the periods 1971–2000, 1981–2010 and 1961–2019 ($p_{(1971-2000)} = 0.002$, $p_{(1981-2010)} < 0.009$, $p_{(1961-2019)} < 0.001$). The highest rate of increase was obtained for the period 1971–2000

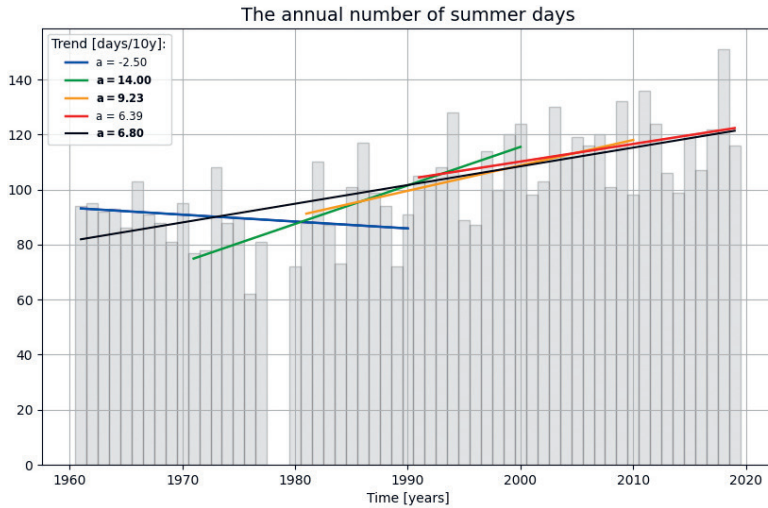


Figure 6. The annual number of summer days for the meteorological station in Dubrovnik with trends for the periods 1961–1990 (blue), 1971–2000 (green), 1981–2010 (orange), 1991–2019 (red) and 1961–2019 (black). In legend are given Sen's slope results (days (10y)⁻¹) and in bold is designated if according to the MK test in a given time statistically significant trend exists.

(14.00 days (10y)⁻¹). After this period, the rates of trend increases were positive but lower, which means that the annual number of summer days was increasing, but more slowly.

The warming of Dubrovnik's climate is evident during the nighttime as well. Thus, the number of tropical nights is increasing (Fig. 7). Except for the period 1961–1990, the MK test shows that significant trends exist in all observed time series, ($p_{(1971-2000)} = 0.007$, $p_{(1981-2010)} < 0.010$, $p_{(1991-2019)} < 0.003$, $p_{(1961-2019)} < 0.001$). Results of Sen's slope show that trends are positive with increasing values for the last two periods (1981–2010 and 1991–2019) indicating that the rise in the annual number of days with a minimum daily temperature higher than 20 °C is accelerated, meaning that nights in Dubrovnik are warming rapidly after the 1970s.

3.2. Satellite data

LST results for the period 2001–2010, show that the lowest value (18.3 °C) of LST is recorded for the sea surface (Fig. 8a). The highest LST is equal to 31.7 °C, and it is obtained for sparsely vegetated areas/bare rock (middle and northwest part of the domain, classes 35 and 36), on discontinuous dense built-up areas, and discontinuous middle-density built-up areas (north part of the domain, classes 1 and 2), and on the business areas (east and middle part of the domain, class 9). Also, relatively higher values of the LST are obtained for the rest of the urban areas, for instance, the old city core (southeast domain, class 7), continuous urban areas (middle west and south part of the domain, classes 1, 2 and 3), business areas (west part of the domain, class 9), public institutions (southwest part of the continental part of the domain, class 11), etc. Except for the sea surfaces and nearby areas, lower values of LST are found in the wooded area (east part

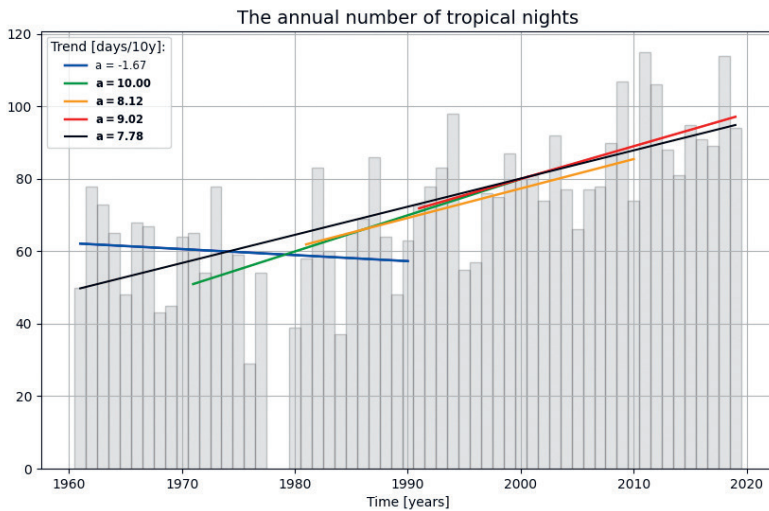


Figure 7. The annual number of tropical nights for the meteorological station in Dubrovnik with trends for the periods 1961–1990 (blue), 1971–2000 (green), 1981–2010 (orange), 1991–2019 (red) and 1961–2019 (black). In legend are given Sen’s slope results (days (10y)⁻¹) and in bold is designated if according to the MK test in a given time statistically significant trend exists.

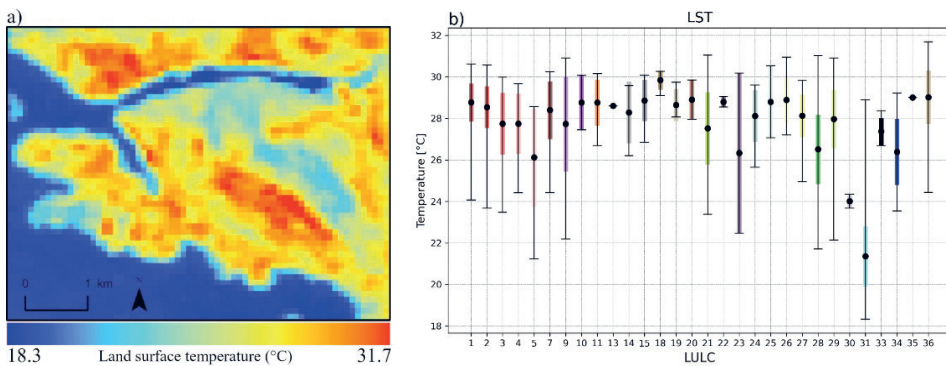


Figure 8. a) The average summer land surface temperature (LST) for the period 2001–2010 obtained from satellite recordings of the LANDSAT5 satellite. b) Graphical representation of average summer LST according to LULC classes with minimum (*bottom line*), mean (*black dot*), and maximum (*top line*) value of average summer LST and respective standard deviation (*coloured*).

of the domain, islands in the west and south part of the domain, west part of the continental domain, class 28) as well.

A more detailed analysis of LST, *i.e.* area-averaged LST according to LULC classes is presented in Fig. 8b. Not only do the mean values of LST show considerable variability between the classes, but also corresponding minimal and maximal values as well as the standard deviations. For instance, the lowest minimum LST, over the land, is obtained for discontinuous very low density urban fabric (class 5), and it equals 21.2 °C. The highest

minimum LST value equals 29.1 °C and is obtained for mine and dump sites (class 18). The lowest maximum LST equals 24.4 °C and is derived for wetlands (class 30, southeast part of domain), while the highest maximum corresponds to bare rock (class 36) and is equal to 31.7 °C. The smallest difference between the maximum and minimum average summer LST equals $\Delta T = 0.5$ °C and is attained for cemeteries (class 22), while the biggest difference over the land is obtained for areas representing forests (class 28) $\Delta T = 9.3$ °C. The lowest mean value of LST value (24.0 °C) is derived for wetlands (class 30), while the highest mean value of LST (29.8 °C) is obtained for mine and dump sites (class 18), this result is quite concerning due to the characteristics of this class (spreading and generating hazardous waste). The smallest standard deviation (0.2 °C) is attained for cemeteries (class 22) and the biggest one (3.9 °C) for sports and leisure facilities with construction (class 23).

3.3. MUKLIMO_3 modelled data

3.3.1. Model validation

Since model simulations provide an approximation of reality, it is necessary to validate simulated data according to measurements. For this purpose, the simulated annual average number of summer days (hereinafter SU) and tropical nights (hereinafter TR), corresponding to the location of the actual meteorological station, were calculated for the period 2001–2010. These results were compared with the results obtained from the measured data. The SU based on the measured data equals 118.8 days, while the model simulates 117.0 days. A relatively small bias of model simulations (1.5%) indicates that model simulations of this cell's SU are quite reliable. On the other side, the bias of model simulations for the TR is greater (14.8%). In the given period, the model simulated 104.3 TR, while according to measurements there were 88.9 such nights. Since the definition of tropical nights is based on minimum temperature, which occurs in the early morning (shortly after sunrise), this result indicates that simulated nights are warmer than they were. Using the same model, the overestimation of climate indices based on minimum temperature is noticed for the city of Vienna as well (Žuvela-Aloise et al., 2016). This result is necessary to investigate further and examine if this overestimation happens persistently and what are the causes for overestimation. One of the possibilities is that nocturnal cooling is not simulated properly, particularly in its connection to the airflow. From that aspect, a more detailed analysis of simulated wind simulations is needed. Since simulations of the summer days are quite reliable, it is reasonable to use the MUKLIMO_3 model for this work. However, analysis and interpretation of nocturnal values should consider its model overestimation. Additionally, in this model validation summer days and tropical nights are calculated using the same criterion as for modelled data in a cuboid method so that measurement and model results are comparable. Although the criterion used in the cuboid method slightly differs from the ETCDDI definition, there was no significant change in the final results of the model validation when the ETCCDI climate index criterion for the measured data was applied (for SD bias was 0.3%, and for TR 18.5%).

3.3.2. Model simulations

Spatial distribution of climate indices, annually-averaged for the period 2001–2010, derived from numerical simulations of the MUKLIMO_3 model, are depicted in Figs.

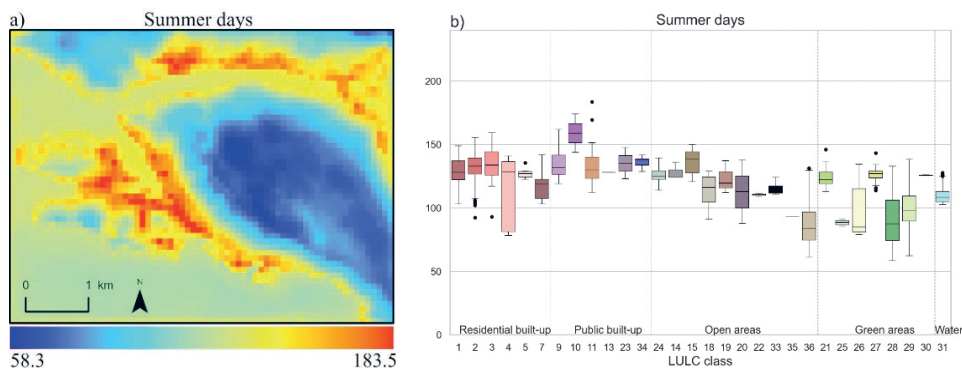


Figure 9. *a)* The annually-averaged number of summer days according to the MUKLIMO_3 simulations for the period 2001–2010. *b)* The annually-averaged number of summer days according to the LULC classes for the period 2001–2010.

9a–12a, while in Figs. 9b–12b results of annually-averaged climate indices are shown according to LULC classification affiliation.

Results of the annually-averaged number of summer days (hereinafter SU) obtained from the model simulations (Fig. 9a) show that the highest number of SU (183.5 days) is occurring in urbanised areas, particularly in the areas situated in the middle of the model domain. The lowest number of SU (58.3 days) regarding the model results is found for natural regions, like forests and bare rock areas. Analysis of SU according to LULC classes shows that on average, heat load in the city is greater in classes of unnatural origin (Fig. 9b), which belong to public built-up, residential built-up and open land LULC groups. From Fig. 9b, it is visible that the model simulates the biggest SU for shopping areas (class 10), after which follows parking areas and garages (class 15), port areas (class 34), sports and leisure facilities with construction (class 23), business area (class 9) and public units (class 11). Heat load is big in residential built-up areas as well, where the greatest SU are obtained for discontinuous medium density urban fabric (class 3). According to the model results, lower SU is obtained for natural domain parts, like meadows and pastures (class 25), agricultural (class 26), forests (class 28), herbaceous vegetation association (class 29) and bare rocks areas (class 36).

The annually-averaged number of hot days (hereinafter HD) obtained from the model simulations has similar spatial distribution as SU, indicating the same areas with the strongest heat load (Fig. 10a). The highest number of HD is perceived in the urbanised part of the model domain (101.9 days), while in the natural areas, these numbers are lower (46.7 days). According to the analysis of LULC classes for HD (Fig. 10b), the heat load is greater in urbanised regions than in natural areas. The highest numbers of HD are obtained for urbanised classes in public built-up, residential built-up and open areas groups. Namely, the greatest HD are simulated for shopping areas (class 10), parking areas and garages (class 15), port areas (class 34), sports and leisure facilities with construction (class 23), business area (class 9) and public units (class 11). The classes corresponding to the vegetated and rocky regions, like meadows and pastures (class 25), agricultural (class 26), forests (class 28), herbaceous vegetation association (class 29), sparsely vegetated areas (class 35) and bare rocks (class 36), show lower heat load.

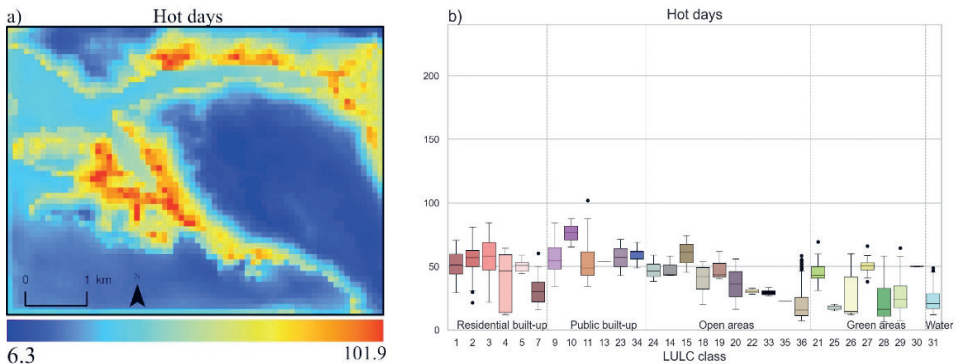


Figure 10. *a)* The annually-averaged number of hot days according to the MUKLIMO_3 simulations for the period 2001–2010. *b)* The annually-averaged number of hot days according to the LULC classes for the period 2001–2010.

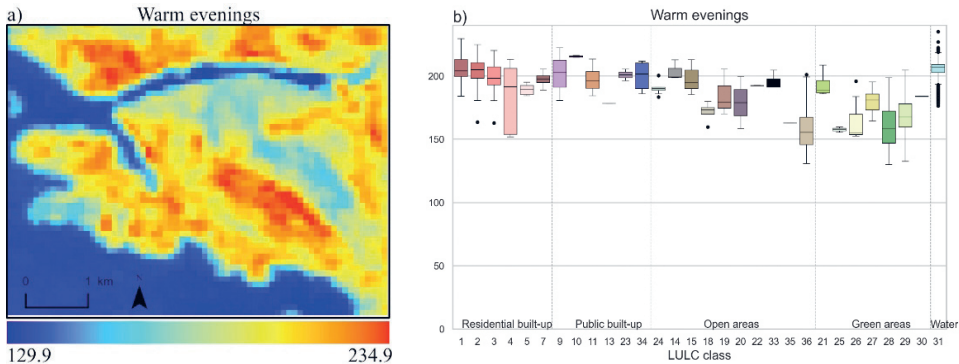


Figure 11. *a)* The annually-averaged number of warm evenings according to the MUKLIMO_3 simulations for the period 2001–2010. *b)* The annually-averaged number of warm evenings according to the LULC classes for the period 2001–2010.

According to the model simulations, heat load over the whole domain is quite strong during the evenings. From Fig. 11a, the spatial distribution of the annually-averaged number of warm evenings (hereinafter WE) is similar to those of SU (Fig. 9a) and HD (Fig. 10a). The highest number of WE are recorded in urban areas (maximum average value is 234.9 days) and the lowest in bare rock and forest regions (129.9 days). As in the previous results, the highest numbers of WE are obtained for unnatural classes of public built-up, residential built-up and open areas groups. For instance, shopping parts (class 10), parking areas and garages (class 15), port areas (class 34), sports and leisure facilities with construction (class 23), business areas (class 9) and public units (class 11) and other residential built-up urbanised classes like continuous urban fabric (class 1), discontinuous dense urban fabric (class 2), discontinuous medium density urban fabric (class 3), old town core (class 7) (Fig. 11b). While heat load in the evenings is on average, according to the model simulations, lower in natural parts of the domain. Precisely, meadows and pastures

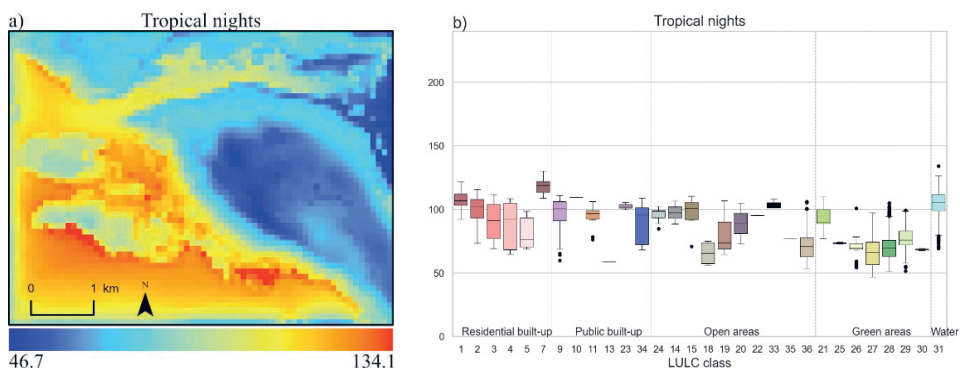


Figure 12. *a)* The annually-averaged number of tropical nights according to the MUKLIMO_3 simulations for the period 2001–2010. *b)* The annually-averaged number of tropical nights according to the LULC classes for the period 2001–2010.

(class 25), agricultural (class 26), forests (class 28), herbaceous vegetation association (class 29), sparsely vegetated areas (class 35) and bare rocks (class 36). But, unlike for the previous two climate indices, the results of HD show that the number of WE is descending with the descent of urban fabric density (classes 1 to 5).

Simulated annually-averaged number of tropical nights (hereinafter TR) shows that the highest number of TR occurs at the sea-land border (south and southwest part of the domain) (Fig. 12a). Similar results for tropical nights in regions close to the water surfaces are obtained in other studies (Žuvela-Aloise, 2017). Domain parts associated with natural areas (such as forests and cliffs) show a lower number of TR. The greatest number of tropical nights over the land is obtained for urbanised areas (the middle part of a domain). Results of TR, shown for each LULC class separately (Fig. 12b), demonstrate that average heat load during the night is stronger in urbanised regions, for example, old town core (class 7), continuous urban fabric (class 1), discontinuous dense urban fabric (class 2), business area (class 9), shopping (class 10), public units (class 11) and parking areas, garages (class 15). As it is expected, classes with vegetation, like classes 25, 26, 27, 28, 29, 30, 35, and 36, have smaller numbers of TR as well as some of the open area classes, like class 18. Furthermore, the presented results reveal that the number of TR depends on the density of built-up urban areas. It is visible from Fig. 12b that a decrease in the mean TR follows a reduction in the density of the built-up regions (classes 1 to 5) similar to what was obtained for WE.

4. Discussion

In this study, results of the observed temperature data, collected at a local meteorological station in the city of Dubrovnik, revealed that temperatures in Dubrovnik have rising trends. Precisely, an analysis of mean daily temperatures for the period 1961–2019 has shown that mean daily temperatures have accelerated rising trends. Similar patterns are found for global surface temperature, for which it is found that each of the last four decades was warmer than the preceding one according to the preindustrial time, 1850–

1900, (IPCC, 2021). Thus, it is evident that global warming is present on a local scale in Dubrovnik as well.

The rise of minimum daily, mean daily and maximum daily temperatures in the period 1961–2019 is the biggest in the JJA season, however, maximum daily JJA temperatures have the highest growth. Besides, it is revealed that in each season, all of the analysed temperatures have ascending trends. Since temperatures in Dubrovnik are already expected to be the highest in the JJA season, this result shows that every year the city is experiencing warmer summers. The rise of minimum and maximum daily temperatures is particularly concerning since exposure to high temperatures could have a negative influence on human health (Nastos and Matzarakis, 2008; Tobias et al., 2010; Matzarakis et al., 2011; Zaninović and Matzarakis, 2014). Except for extreme daily temperatures and mean daily temperature results, analysis of the climate indices of the annual number of summer days and tropical nights, calculated from the observed temperature data, shows that these climate indices have rising trends as well. Similar trends of summer days are recorded in some other studies, for instance at the meteorological station in Zagreb (Nimac et al., 2021). Rising trends of these climate indices indicate that the maximum daily temperature in Dubrovnik is increasing and that the minimum daily temperature is increasing, but rapidly. Intensified nocturnal heating of the town can be very uncomfortable since the city cannot cool even at night, which prolongs exposure to high temperatures, enhances energetics and water demands, etc.

The use of model and satellite data provided insight into the spatial distribution of the heat load. From the satellite data results, it follows that in summer, rocky areas, sparsely vegetated areas, and urbanised built-up areas are heated the most, which is according to their material characteristics (such as heat capacity, albedo, emissivity, reflexivity) expected. Considering that LANDSAT5 satellite data was recording always at about 10:40 a.m. (GMT+2) and that in the morning, rural areas heat up faster than urban areas (Masson et al., 2020), it is not surprising that the highest LST values are recorded for bare rocks areas (Fig. 8a). Higher values of LST are recorded in urbanised parts as well, but slightly lower than in bare rock areas, which belong to open land parts of the domain. In open land areas in comparison to built-up parts of the city, shading effects, which contribute to the mitigation of heating, are missing. Lower values of LST are recorded in vegetated parts, in which through shading effects and evapotranspiration processes, self-cooling is enhanced (Masson et al., 2020). However, results presented according to LULC classes have revealed big standard deviations for some classes, for example, classes 23, 5, and 9. In this case, a bigger standard deviation represents bigger LST spatial variability of a certain LULC class, while a smaller standard deviation means that for some classes similar LST values are recorded over the whole domain. The bigger spatial variability of some classes could be a consequence of two different effects. Either that class encompasses regions with different properties, which cause different LST values for the same class (in that case, maybe redefinition of classes should be applied to improve properties of a certain class) or that classes have relatively homogenous properties, but differences in LST values are the product of different environmental impacts and their processes (for instance, shading effects, advection influence, cooling processes of neighbour areas...). These possibilities should be more examined in further research to improve the understanding of interaction processes between certain LULC classes and their surroundings.

MUKLIMO_3 model simulations indicate that in general heat load in the city of Dubrovnik, during the day, is greatest in the public built-up group classes, particularly in shopping areas, for which the highest values of SU, HD and WE are obtained. After public built-up group classes, a bigger heat load is simulated for urbanised classes from residential built-up and open areas groups. These results are in accordance with so far findings that urbanised parts of the city are heating up more than natural surrounding rural areas, mainly due to the artificialization of the surface (Oke, 2017). The main difference in warming of surface temperature in rural and urban areas is mainly a consequence of evapotranspiration and convection efficiency differences among these regions (Manoli et al., 2019). In all analysed climate indices, it is visible that heat load is lower in classes of natural origin, grouped in open land and green areas (classes 25, 26, 28, 29 and 36). In these places, vegetation, like forests, and bushy vegetation, enhance cooling effects through the shading effects and evapotranspiration processes, also the evaporation processes in moist soils, typical for forests, contribute to the mitigation of surface temperature (Masson et al., 2020). Nevertheless, in the green area group of LULC classes, parks (green urban areas, class 25) stands out from the other classes. Here the MUKLIMO_3 model simulates higher values of climate indices, particularly for WE and TR. It could be concluded that, even though in parks there are cooling effects from vegetation and shading, because of heat absorbed in its urbanised surroundings, these cooling effects are diminished during the nighttime when heat is emitted from the surroundings. However, it is found in Texas that the lack of greenery parts of the city, *i.e.* a high fraction of areas covered mostly by concrete surfaces of buildings has a negative impact on health risks, while green urban parts contribute significantly to the reduction of health risks (Chun et al., 2021). In the residential built-up group of classes, it is interesting to notice that for climate indices SU and HD (day-time indices) the biggest heat load is simulated for discontinuous medium density urban fabric (class 3), while classes with a bigger density of urban fabric (classes 1 and 2) have lower heat load. During the nighttime, results are the opposite, according to the results of WE and TR, it is visible that heat load is reduced with the decrease of built-up density. Some studies (Kakoniti et al., 2016) show that in dry climates, which could be linked with the climate in the city of Dubrovnik, sparser geometry of urban canyons, like here class 3, does not guarantee lower surface temperatures. In sparser parts of the city, during the day, surface temperatures are higher, while there are more surfaces under direct solar radiation and there are no shading effects like in denser urbanised parts. During the night, when direct solar radiation is missing, heat absorbed in dense parts of the city is released and limits radiation cooling causing additional warming of these parts of the city at night (Masson et al., 2020). These effects are specifically evident in the old town core (class 7), which according to the TR results has the greatest heat load during the nighttime. In old town core ventilation processes, and therefore cooling effects, are reduced due to very narrow streets and because of old city walls. It is interesting to notice that the model simulates less TR for urbanised parts of the city, situated in the northern part of the model domain than for the urbanised parts of the city in the middle of the domain. This northern urbanised part of the city is not widely distributed and it is surrounded by mountains and sea, where land-sea and mountain-valley breeze circulation are in superposition (Fig. 1a). This result indicates the importance of the position in the city as well as the influence of the surroundings. However, these effects should be more investigated in future.

Despite the model overestimating the number of TR, this work aimed to investigate some general patterns of heat load spatial distribution at night and during the day in the

city of Dubrovnik. Results of climate indices according to LULC classes are collectively demonstrated using box plots for each LULC class to present all simulated values of a particular LULC class. Since LULC classes are distributed unequally across the domain, domain parts belonging to the same LULC class may be subject to various local and surrounding influences depending on their position, for example, proximity to the sea, mountain barriers, shading, and so on. Therefore, to understand the heat load patterns of certain classes better, a more detailed analysis of heat load and factors that affect it depending on the position and surroundings of LULC classes are needed in future research, especially here, in the Mediterranean region, where it is found that urban morphology has one of the greatest impacts on UHI intensity (Salvati et al., 2017).

5. Conclusions

In this study, characteristics of temperature and heat load are investigated for the city of Dubrovnik, Croatia, using measured, modelled and satellite data. Trends of measured temperature-related elements (mean daily temperatures, mean seasonal temperatures, mean seasonal maximum and minimum daily temperatures) and climate indices (summer days and tropical nights) share similar characteristics indicating significant warming of the city, which is the strongest for the summer (JJA) season, particularly for maximum daily temperatures, which have the highest increase in the observed period. Climate indices based on measurements (summer days and tropical nights) uphold the abovementioned conclusion about the warming of the city. Furthermore, results show strong warming not only during the daytime but also during the night. These results indicate thermal discomfort in the city of Dubrovnik that can be particularly enhanced during the summer. In addition, there are many other unwanted consequences related to increased heat load (ecological consequences, negative impact on tourism, adverse effect on public health and quality of life, increased risk of wildfires, increased energy and water demands etc.).

The cooling effect of vegetation and natural surfaces is reflected in both satellite and modelled data. Furthermore, MUKLIMO_3 model simulations showed that urbanised areas affect the spatial distribution of the heat load in the city with generally stronger urban heat load in urbanized than in natural areas. Obtained results underline the importance of protecting natural areas in the city and the need for considering the heat load distribution while preparing urban plans. In this work, the average state of the heat load distribution was obtained as an overall result of many different local and global processes. The city of Dubrovnik is exposed to global warming as are other cities worldwide, but its configuration, building materials and local meteorological influences can mitigate or enhance the heat load, and they certainly affect its spatial distribution. Hence, possibilities of heat mitigation, and particular conditions that support extreme heat load in the city would be valuable to investigate in further research. Additionally, it would be interesting and worthwhile to apply this approach to investigate the heat load of other Mediterranean cities, compare the results and examine the influence of different morphological city structures on the heat load in similar climate conditions. Also, the impact of global modes of climate variability, like North Atlantic Oscillation (NAO) which strongly affects weather conditions in Europe, could modify thermal conditions in the city.

Acknowledgements – This research was funded by the Klima-4HR project (KK.05.1.1.02.0006). We would like to thank the Meteorological and Hydrological Service, Zagreb, Croatia for providing the measured data.

References

- Balling, R. C., Cerverny, R. S. and Idso, C. D. (2001): Does the urban CO₂ dome of Phoenix, Arizona contribute to its heat island?, *Geophys. Res. Lett.*, **28**, 4599–4601, <https://doi.org/10.1029/2000GL012632>.
- Chun, B., Hur, M. and Won, J. (2021): Impacts of thermal environments on health risk: A case study of Harris County, Texas, *Int. J. Environ. Res. Public Health*, **18**, 5531, <https://doi.org/10.3390/IJERPH18115531>.
- Climdex (2020): <https://www.climdex.org/learn/indices/>
- Früh, B., Becker, P., Deutschländer, T., Hessel, J. D., Kossmann, M., Mieskes, I., Namyslo, J., Roos, M., Sievers, U., Steigerwald, T., Turauf, H. and Wienert, U. (2011): Estimation of climate-change impacts on the urban heat load using an urban climate model and regional climate projections, *J. Appl. Meteorol. Climatol.*, **50**, 167–184, <https://doi.org/10.1175/2010JAMC2377.1>.
- Giorgi, F. (2006): Climate change hot-spots, *Geophys. Res. Lett.*, **33**, 8707, <https://doi.org/10.1029/2006GL025734>.
- Graczyk, D., Pińskwar, I., Kundzewicz, Z. W., Hov, Ø., Førland, E. J., Szwed, M. and Choryński, A. (2017): The heat goes on — Changes in indices of hot extremes in Poland, *Theor. Appl. Climatol.*, **129**, 459–471, <https://doi.org/10.1007/s00704-016-1786-x>.
- Grbec, B., Matić, F., Beg Paklar, G., Morović, M., Popović, R. and Vilibić, I. (2018): Long-term trends, variability and extremes of in situ sea surface temperature measured along the Eastern Adriatic coast and its relationship to hemispheric processes, *Pure Appl. Geophys.*, **175**, 4031–4046, <https://doi.org/10.1007/S00024-018-1793-1>.
- IPCC (2021): Summary for policymakers, in: *Climate Change 2021: The Physical Science Basis. Contribution of Working Group I to the Sixth Assessment Report of the Intergovernmental Panel on Climate Change*, edited by Masson-Delmotte, V., Zhai, P., Pirani, A., Connors, S. L., Péan, C., Berger, S., Caud, N., Chen, Y., Goldfarb, L., Gomis, M. I., Huang, M., Leitzell, K., Lonnoy, E., Matthews, J. B. R., Maycock, T. K., Waterfield, T., Yelekçi, O., Yu, R. and Zhou. Cambridge University Press, Cambridge, United Kingdom and New York, NY, USA, pp. 3–32, https://www.ipcc.ch/report/ar6/wg1/downloads/report/IPCC_AR6_WGI_SPM.pdf.
- Jopp, R., Delacy, T. and Mair, J. (2010): Developing a framework for regional destination adaptation to climate change, *Current Issues in Tourism*, **13**, 591–605, <https://doi.org/10.1080/13683501003653379>.
- Kakoniti, A., Georgiou, G., Marakkos, K., Kumar, P. and Neophytou, M. K. A. (2016): The role of materials selection in the urban heat island effect in dry mid-latitude climates, *Environ. Fluid Mech.*, **16**, 347–371, <https://doi.org/10.1007/s10652-015-9426-z>.
- Kendall, M. G. (1975): *Rank correlation methods*. Griffin, London.
- Klaić, Z. B., Nitis, T., Kos, I. and Moussiopoulos, N. (2002): Modification of the local winds due to hypothetical urbanization of the Zagreb surroundings, *Meteorol. Atmos. Phys.*, **79**, 1–12, <https://doi.org/10.1007/S703-002-8225-Z>.
- Mann, H. B. (1945): Nonparametric tests against trend, *Econometrica*, **13**, 245–259, <https://doi.org/10.2307/1907187>.
- Manoli, G., Fatichi, S., Schläpfer, M., Yu, K., Crowther, T. W., Meili, N., Burlando, P., Katul, G. G. and Bou-Zeid, E. (2019): Magnitude of urban heat islands largely explained by climate and population, *Nature*, **573**, 55–60, <https://doi.org/10.1038/s41586-019-1512-9>.
- Masson, V., Lemonsu, A., Hidalgo, J. and Voogt, J. (2020): Urban Climates and Climate Change, *Ann. Rev. Environ. Res.*, **45**, 411–444, <https://doi.org/10.1146/annurev-environ-012320-083623>.
- Matzarakis, A., Muthers, S. and Koch, E. (2011): Human biometeorological evaluation of heat-related mortality in Vienna, *Theor. Appl. Climatol.*, **105**, 1–10, <https://doi.org/10.1007/S00704-010-0372-X>.

- Nastos, P. T. and Matzarakis, A. (2008): Human-biometeorological effects on sleep disturbances in Athens, Greece: A preliminary evaluation, *Indoor Built Environ.*, **17**, 535–542, <https://doi.org/10.1177/1420326X08097706>.
- Nimac, I., Herceg-Bulić, I., Žuvela-Aloise, M. and Žgela, M. (2022): Impact of North Atlantic Oscillation and drought conditions on summer urban heat load - A case study for Zagreb, *Int. J. Climatol.*, **42**, 4850–4867, <https://doi.org/10.1002/JOC.7507>.
- Nimac, I., Herceg-Bulić, I., Cindrić Kalin, K. and Perčec Tadić, M. (2021): Changes in extreme air temperatures in the mid-sized European city situated on southern base of a mountain (Zagreb, Croatia), *Theor. Appl. Climatol.*, **146**, 429–441, <https://doi.org/10.1007/s00704-021-03689-8>.
- Nimac, I. and Perčec Tadić, M. (2017): Complete and homogeneous monthly air temperature series for the construction of 1981–2010 climatological normals in Croatia, *Geofizika*, **34**, 225–249, <https://doi.org/10.15233/gfz.2017.34.13>.
- Oke, T. R., Mills, G., Christen, A. and Voogt, J. A. (2017): *Urban climates*. Cambridge University Press, Cambridge, New York, Port Melbourne, Daryaganj, Singapore, **2**, 197–202 pp.
- Pandžić, K. and Likso, T. (2010): Homogeneity of average annual air temperature time series for Croatia, *Int. J. Climatol.*, **30**, 1215–1225, <https://doi.org/10.1002/JOC.1922>.
- Salvati, A., Palme, M. and Inostroza, L. (2017): Key parameters for urban heat island assessment in a Mediterranean context: A sensitivity analysis using the urban weather generator model, *IOP Conf. Ser. Mater. Sci. Eng.*, **245**, 082055, <https://doi.org/10.1088/1757-899X/245/8/082055>.
- Sen, P. K. (1968) Estimates of the regression coefficient based on Kendall's tau, *JASA*, **63**, 1379–1389, <https://doi.org/10.1080/01621459.1968.10480934>.
- Sievers, U. (1995): Verallgemeinerung der Stromfunktionsmethode auf drei Dimensionen (Generalization of the streamfunction/vorticity method to three dimension), *Meteorol. Z.*, **3**, 3–15, <https://doi.org/10.1127/metz/4/1995/3>.
- Sievers, U. (1990): *Dreidimensionale Simulationen in Stadtgebieten*. Umwelt-meteorologie, Schriftenreihe Band 15: Sitzung des Hauptausschusses II am 7. und 8. Juni in Lahnstein. Kommission Reinhaltung der Luft im VDI und DIN, Dusseldorf. S. 92–105 (in German).
- Sievers, U. and Zdankowski, W. (1986): A microscale urban climate model, *Contr. Phys. Atmosph.*, **59**, 13–40.
- Sobrinho, J. A., Jiménez-Muñoz, J. C. and Paolini, L. (2004): Land surface temperature retrieval from LANDSAT TM 5, *Remote Sens. Environ.*, **90**, 434–440, <https://doi.org/10.1016/J.RSE.2004.02.003>.
- Tan, J., Zheng, Y., Tang, X., Guo, C., Li, L., Song, G., Zhen, X., Yuan, D., Kalkstein, A. J., Li, F. and Chen, H. (2010): The urban heat island and its impact on heat waves and human health in Shanghai, *Int. J. Biometeorol.*, **54**, 75–84, <https://doi.org/10.1007/S00484-009-0256-X>.
- Tobías, A., de Olalla, P. G., Linares, C., Bleda, M. J., Caylà, J. A. and Díaz, J. (2010): Short-term effects of extreme hot summer temperatures on total daily mortality in Barcelona, Spain, *Int. J. Biometeorol.*, **54**, 115–117, <https://doi.org/10.1007/S00484-009-0266-8>.
- United Nations, Department of Economic and Social Affairs, Population Division (2019): *World Urbanization Prospects: The 2018 Revision (ST/ESA/SER.A/420)*. New York: United Nations.
- Vilibić, I., Šepić, J. and Proust, N. (2013): Weakening thermohaline circulation in the Adriatic Sea, *Clim. Res.*, **55**, 217–225, <https://doi.org/10.3354/CR01128>.
- Zaninović, K., Gajić-Čapka, M., Tadić, M. P., Vučetić, M., Milković, J., Bajić, A., Cindrić, K., Cvitan, L., Katušić, Z., Kaučić, D., Likso, T., Lončar, E., Lončar, Ž., Mihajlović, D., Pandžić, K., Patarčić, M., Srnc, L. and Vučetić, V. (2008): *Klimatski atlas Hrvatske / Climate atlas of Croatia 1961–1990, 1971–2000*. Državni hidrometeorološki zavod, Zagreb, 200 pp.
- Zaninović, K. and Matzarakis, A. (2014): Impact of heat waves on mortality in Croatia, *Int. J. Biometeorol.*, **58**, 1135–1145, <https://doi.org/10.1007/S00484-013-0706-3>.
- Žuvela-Aloise, M., (2017): Enhancement of urban heat load through social inequalities on an example of a fictional City King's Landing, *Int. J. Biometeorol.*, **61**, 527–539, <https://doi.org/10.1007/s00484-016-1230-z>.

- Žuvela-Aloise, M., Koch, R., Buchholz, S. and Früh, B. (2016): Modelling the potential of green and blue infrastructure to reduce urban heat load in the City of Vienna, *Clim. Change*, **135**, 425–438, <https://doi.org/10.1007/s10584-016-1596-2>.
- Žuvela-Aloise, M., Koch, R., Neureiter, A., Böhm, R. and Buchholz, S. (2014): Reconstructing urban climate of Vienna based on historical maps dating to the early instrumental period, *Urban Clim.*, **10**, 490–508, <https://doi.org/10.1016/J.UCLIM.2014.04.002>.
- World Meteorological Organization (2004): Report of the CCI/CLIVAR Expert Team on Climate Change Detection, Monitoring and Indices (ETCCDMI), https://library.wmo.int/index.php?lvl=notice_display&id=11636#.Y6MMzXbMJAR.

SAŽETAK

Temperатурне карактеристике и toplinsko opterećenje Dubrovnika

Marijana Boras, Ivana Herceg-Bulić, Matej Žgela i Irena Nimac

U ovom radu istraživane su temperатурне карактеристике i toplinsko opterećenje Dubrovnika korištenjem podataka o temperaturi izmjerenima na lokalnoj meteorološkoj postaji u Dubrovniku u razdoblju 1961.–2019., satelitskih podataka prikupljenih satelitom LANDSAT5 u razdoblju 2001.–2010. te podataka klimatskih indeksa, dobivenih simulacijama urbanog klimatskog modela (MUKLIMO_3) za razdoblje 2001.–2010. Trendovi srednjih dnevnih, maksimalnih i minimalnih dnevnih te sezonskih temperatura analizirani su korištenjem Senovog nagiba i Mann-Kendallovog testa. Sve analize pokazuju uzlazne trendove promatranih temperatura. Međutim, pokazuje se da je porast temperatura najveći u ljetnoj sezoni, posebice za maksimalne dnevne temperature, za koje je zabilježen najveći porast. Isti pristup primijenjen je za ispitivanje klimatskih indeksa (ljetni dani i tropske noći), koji ukazuju na porast godišnjih brojeva ljetnih dana i tropskih noći. Rezultati satelitskih podataka prosječne ljetne površinske temperature u razdoblju 2001.–2010. pokazuju da se područja golih stijena i urbanizirani dijelovi domene jače zagrijevaju od područja s vegetacijom. Klimatski indeksi (ljetni dani, vrući dani, tople večeri i tropske noći) dobiveni simulacijama urbanog klimatskog modela MUKLIMO_3 također ukazuju da se u prosjeku u Dubrovniku urbanizirane površine više zagrijevaju od prirodnih površina s vegetacijom te da se noćno toplinsko opterećenje smanjuje sa smanjenjem gustoće izgrađenosti.

Ključne riječi: temperatura, toplinsko opterećenje, urbana klima, Senov nagib, Mann-Kendallov test, klimatski indeksi, model MUKLIMO_3, satelit LANDSAT5

Corresponding author's address: Ivana Herceg-Bulić, Department of Geophysics, Faculty of Science, University of Zagreb, Horvatovac 95, HR-10000 Zagreb, Croatia; tel: +385 1 460 5932; e-mail: ivana.herceg.bulic@gfz.hr



This work is licensed under a Creative Commons Attribution-NonCommercial 4.0 International License.